Review | Open Access

Advanced Energy Conversion

Samsalee *et al. Adv. Energy Convers.* **2026**, *1*, 9 **DOI:**10.20517/aec.2026.20

Hydrothermal carbonization of agri-food waste to carbon dot nanofluids

Namfon Samsalee[1], Rungsinee Sothornvit[2], Kanit Manatura[3,4]

Keywords:
Agri-food waste valorization, carbon dots, hydrothermal carbonization, thermal nanofluids, machine learning, nanofluid stability

Citation: Samsalee, N.; Sothornvit, R.; Manatura, K. Hydrothermal carbonization of agri-food waste to carbon dot nanofluids. *Adv. Energy Convers.* **2026**, *1*, 9. https://dx.doi.org/10.20517/aec.2026.20

Received: 17 Jun 2026
First Decision: 4 Aug 2026
Revised: 18 Sep 2026
Accepted: 22 Sep 2026
Published: 29 Sep 2026

Academic Editor: Wei-Mon Yan
Copy Editor: Shu-Yuan Duan
Production Editor: Shu-Yuan Duan

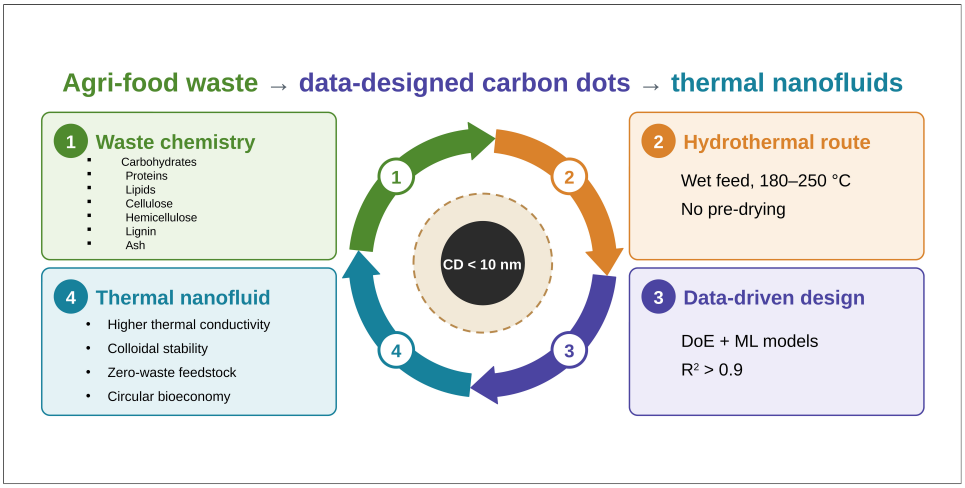

Abstract

Considering challenges related to increasing agri-food waste (AFW), circular bioeconomy approaches are needed to tackle conventional disposal or low-value energy recovery. We report a comparative evaluation of upcycling AFW into carbon dots (CDs) via thermochemical conversion for the sustainable replacement of toxic, petroleum-based nanoparticles in energy applications. We focus on the key factors of hydrothermal carbonization over dry torrefaction, such as higher energy efficiency for high moisture content and higher oxygen functionalization. The review discusses how these affect the molecular hydrolysis and aromatization pathways to yield CDs. This includes the structural taxonomy of AFW-derived CDs, such as graphene dots, CDs, and carbonized polymer dots. We discuss the core-shell structure underlying the thermal transport and colloidal stability of AFW-derived CDs. Next, we summarize our proposed data-driven approach that combines statistical design of experiments with machine learning. In previous studies, these two methods successfully predicted the properties of CDs with coefficient of

[1]Department of Applied Biology, Faculty of Sciences and Liberal Arts, Rajamangala University of Technology Isan, Nakhon Ratchasima 30000, Thailand.
[2]Department of Food Engineering, Faculty of Engineering at Kamphaengsaen, Kasetsart University, Kamphaeng Saen Campus, Nakhon Pathom 73140, Thailand
[3]Department of Mechatronics Engineering, Faculty of Engineering and Technology, Rajamangala University of Technology Isan, Nakhon Ratchasima 30000, Thailand.
[4]Sustainable Development and Intelligent Systems Research Unit, Faculty of Engineering and Technology, Rajamangala University of Technology Isan, Nakhon Ratchasima 30000, Thailand.

Correspondence to: Dr. Kanit Manatura, Department of Mechatronics Engineering, Faculty of Engineering and Technology, Rajamangala University of Technology Isan, Nakhon Ratchasima 30000, Thailand. E-mail: kanit.ma@rmuti.ac.th

determination (R^2) = 0.90-0.9996 with varying degrees of accuracy dependent on the size of the datasets used. However, their generalizability outside the domain of data sampling used in each study was unclear. Depending on the base fluid, CD precursor, and loading, thermal conductivity improvements of 11%-175% were reported. Colloidal stability exceeded 30 days with functionalized CDs. This property addresses the agglomeration and sedimentation issues for high-performance thermal nanofluids. Finally, we summarize the key barriers for upscaling and conducting life cycle assessment studies while providing an outlook toward commercialization of intelligent waste-derived nanofluids for next-generation solar-thermal and advanced heat-transfer technologies.

INTRODUCTION

Global agri-food waste (AFW), including agricultural residues and food waste from consumers, represents a serious threat to sustainable development[1]. Traditional practices such as landfilling and incineration cause huge losses of valuable chemical energy of the biomass and contribute significantly to greenhouse gas (GHG) emissions[2]. A paradigm shift to transform AFW into advanced high-value products through the circular economy and Bio-Circular-Green (BCG) principles is urgently needed[3]. Recently, carbon dots (CDs) have emerged as promising candidates for the next generation of energy materials, particularly in thermal nanofluids. In previous studies, carbon additives such as carbon nanotubes (CNTs) and graphene were used to improve the thermal conductivity of the base fluid. However, their agglomeration and sedimentation were significant problems due to the strong van der Waals interaction[4].

In another study, the small size and numerous surface groups on CDs with excellent intrinsic colloidal stability were used to formulate novel, ultra-stable thermal nanofluids[5]. CDs are usually smaller than 10 nm in size with rich surface functional groups (such as hydroxyl, carboxyl, and amino). To date, there are three main gaps that limit this field. First, there is little consideration of AFW's inherent complexity [i.e., the mixture of varying amounts of carbohydrates, proteins, and lipids all hydrolyzed, dehydrated, and aromatized simultaneously in hydrothermal carbonization (HTC)][6] [Figure 1].

Most works describe a result obtained using only one precursor type at a given set of conditions. These results are often non-transferable between different feedstocks. Second, the vast majority of published work still focuses on empirical, one-factor-at-a-time (OFAT) optimization that does not consider the interaction between reaction parameters, which results in uncontrolled reaction severity and poorly controlled graphitic structures[7]. Third, and perhaps the most important limitation, is that none of these works considers both precursor composition and synthesis parameters to generate the desired macroscopic thermal-fluid properties within the same framework. This means that each step is optimized independently; for example, a set of synthesis conditions may be shown to be optimal for a target property such as CD yield or fluorescence but not necessarily the actual increase in thermal conductivity that will govern the usefulness of AFW.

The present review intends to fill these three gaps by introducing a strategic engineering approach to the synthesis of AFW-derived CDs. The approach transforms the empirical, trial-and-error process into an optimized, data-driven one, including both precursor composition and synthesis conditions as well as thermal-fluid performance. This review evaluates the potential of using statistical design of experiments (DoE), namely the Taguchi method and response surface methodology (RSM), to fine-tune the properties of the CDs[8]. We also intend to discuss the use of machine learning (ML) as a powerful tool to predict the thermophysical behavior of the resulting optimized nanostructures, saving money and time through fewer experimental trials[9].

This review is structured as follows: Section **FOOD WASTE VALORIZATION VIA THERMOCHEMICAL ROUTES** examines AFW composition and thermochemical conversion routes; Section **DATA-DRIVEN FRAMEWORK FOR INTELLIGENT CD SYNTHESIS AND NANOFLUID FORMULATION**; Section **ADVANCED THERMAL NANOFLUIDS INTEGRATED WITH CDS** analyzes heat-transfer enhancement mechanisms in CD-based nanofluids; Section **ENVIRONMENTAL IMPACT AND PRACTICAL CHALLENGES** addresses environmental impact, scalability, and

Figure 1. Concept to produce carbon dots by hydrothermal carbonization. The specific graphic icons used in Figure 1 (representing the agri-food waste raw material, the test tube, and the black carbon dots) were obtained from Canva (https://www.canva.com) under the platform's 'Free' user license.

techno-economic considerations; and Section CONCLUSION provides conclusions and a future research roadmap.

FOOD WASTE VALORIZATION VIA THERMOCHEMICAL ROUTES

Compositional synergy: carbohydrates, proteins, and lipids as precursors

"Agri-food waste" is defined as inedible or wasteful plant- and animal-based products such as fruit and vegetable peels, spent grains, shells, and post-consumer food wastes. The organic components of the various AFW streams reported in Table 1 consist largely of lignocellulosic fractions, including cellulose (11-65 wt.%), hemicellulose (6-50 wt.%), and lignin (3-36 wt.%), with each macromolecule determining its specific mechanism for creating carbon nanostructures. The chemical composition of AFW affects CQD formation and properties. Carbohydrates, in particular, are considered superior carbon sources for carbon quantum dot (CQD) synthesis due to their chemical structure, high carbon content, and distinct thermal decomposition behavior. Natural polymers present in AFW, such as cellulose, hemicellulose, and lignin, provide a rich carbon framework that readily converts into nanostructured carbon materials under thermal treatment[2,7]. For example, rice straw and nut shells are commonly used agricultural byproducts, which provide the main carbon backbone by the dehydration and polymerization of cellulose and hemicellulose[10,11]. On the other hand, the proteins and lipids in food waste are an inherent source of nitrogen, providing *in situ* self-doping that results in improved surface reactivity and polarity of CDs, avoiding the use of high-cost external dopants[12]. Residual lipids play an important role in modulating the surface hydrophobic-hydrophilic balance. This is crucial for preventing particles from agglomerating in order to guarantee ultra-long-term colloidal stability when they are dispersed in different thermal base fluids [7]. Finally, the combined composition enables the engineering of CDs with a desired surface chemistry based on the molecular structure of the starting material. The typical physicochemical characteristics of various AFW precursors providing a rich carbon framework are summarized in Table 1.

Carbon dots taxonomy

The key to developing CDs for high-performance thermal fluids lies in understanding their basic structural classifications and inherent physics. CDs

Table 1. Physicochemical properties of selected AFW precursors for CD synthesis

Wastes	Lignocellulosic and ash contents (wt.%)				Ultimate analysis (wt.%)				References
	Cellulose	Hemicellulose	Lignin	Ash	C	H	O	N	
Rice straw	-	-	-	9.31	34.47	5.84	58.82	0.87	[10]
Almond hull	13.38	24.06	11.41	-	41.26	5.71	52.16	0.86	[13]
Cassava peels	11.30	22.39	3.09	-	41.63	6.11	50.85	1.57	[13]
Sugarcane bagasse	-	-	-	2.17	46.37	6.29	46.79	0.55	[14]
Walnut shells	31.40	45.30	19.20	5.09	45.77	9.05	44.2	0.84	[11]
Groundnut shells	26.70	31.50	16.50	25.26	39.84	7.25	51.87	0.88	[11]
Melon seed shells	30.00	29.60	18.90	7.27	71.49	9.63	16.92	1.86	[11]
Spent coffee grounds	-	-	-	2.25	46.98	7.49	45.30	0.22	[15]
Tea waste	-	-	-	3.03	46.23	6.99	46.56	0.22	[15]
Durian peels	50-60	30.70	13.60	-	-	-	-	-	[16]
Banana peels	60-65	6-8	5-10	-	-	-	-	-	[17]
Mango seed husk	49.99	21.15	25.53	0.91	45.90	6.03	46.80	0.50	[17]
Coconut shells	30.58	26.70	33.30	10.52	50.25	5.70	42.57	0.71	[18]
Corncob residue	50-60	-	20-30	-	68.89	-	29.88	1.23	[19]
Mango peels	34.8	50.5	14.7	12.5	37.41	6.9	52.74	2.69	[20]
Orange peels	-	-	-	2.00	46.42	8.00	44.56	0.44	[21]
Passion fruit peels	28.58	23.01	36.16	5.71	-	-	-	-	[22]
Banana stalk	47.0	28.0	20.0	19.0	33.0	4.3	60.5	1.9	[23]

- = parameter not reported in the cited source. All lignocellulosic and ultimate-analysis values are expressed on a dry basis (wt%). Values are reported as single figures or as ranges according to how each cited source reported them; ranges are not measurement uncertainty and are not converted to a midpoint.

fall broadly within the general class of zero-dimensional (0D) carbonaceous nanomaterials. However, they do not represent a monolithic family of materials. Rather, according to their carbonization level within the individual structure and precursor source, they can be classified into three main structural classes for taxonomic purposes: (i) graphene dots (GDs), composed of one or few layer sheets of graphene with clearly defined sp^2 crystalline domains; (ii) carbon dots (CDs), which are spherical nanoparticles with a graphitic core that is dislocated yet linked locally with localized quantum confinement; and (iii) carbonized polymer dots (CPDs), composed of deep cross-linked amorphous polymeric chains without well-defined structured crystalline networks[12,24,25].

Morphologically, HTC-derived CDs prepared from biomass through subcritical liquid transformation follow a core-shell structure: a core consisting of carbonized sp^2-hybridized clusters responsible for electron flow and primary density, surrounded by a shell that is amorphous, defective, and filled with functional groups derived from the original food waste[18,19]. When employing these structures for thermal fluid applications, the most important design consideration is to maintain an optimum balance between the degree of graphitization in the core (responsible for intrinsic heat conduction) and the passivating effect in the shell (responsible for fluid colloidal stability). HTC of heterogeneous AFW leads to CPDs since cross-linking polymerization prevails during the subcritical aqueous reaction pathway. This review focuses largely on CPD-type CDs, unless otherwise noted, although changing synthesis parameters allows tuning the product distribution toward more graphitized CD-type products.

Comparative analysis of dry torrefaction *vs.* HTC

The selection of the appropriate thermochemical process is key to determining the ultimate shape and surface properties of carbonaceous products. Dry torrefaction involves conventional heating at temperatures of 200-300 °C in an inert atmosphere, aimed at eliminating moisture and volatiles from the feed-

Table 2. Comparative analysis of dry torrefaction and HTC for biomass valorization and CD synthesis

Parameters	Dry torrefaction[10]	HTC[11,15]
Operating conditions	200-300 °C, inert atmosphere (N_2)	180-250 °C, subcritical aqueous medium (autogenous pressure)
Reaction mechanisms	Dehydration, devolatilization, and solid-state cross-linking	Hydrolysis, dehydration, decarboxylation, and polymerization
Energy efficiency	Low for wet biomass (requires highly energy-intensive pre-drying)	High (ideal for high-moisture AFW; no pre-drying required)
Carbon dimensionality	Bulk, three-dimensional (3D) macrostructures	Zero-dimensional (0D) nanoparticles (< 10 nm) and functionalized hydrochars
Surface functionalization	Poor (hydrophobic, low oxygen functional groups)	Excellent (rich in -OH, -COOH groups promoting hydrophilicity and stability)
Suitability for CD synthesis	Low: produces non-dispersible carbon blocks	Favorable: liquid-mediated nucleation allows precise size control and auto-passivation

HTC: Hydrothermal carbonization; CD: carbon dot.

stock, which results in high-calorific solid biofuels (torrefied biomass)[10]. This solid-state transformation produces bulk, non-dispersible, hydrophobic macro-carbon structures, which are not suitable for stable colloidal suspensions.

In contrast, HTC takes place in a subcritical water medium and enables liquid-mediated reaction kinetics favorable for CD production. The HTC temperature (180-250 °C) range is similar to that of dry torrefaction; however, it occurs in an aqueous subcritical system that enables liquid-mediated nucleation instead of solid-state carbonization. In this aqueous, high-pressure medium, AFW macromolecules are rapidly hydrolyzed into reactive monomeric units. The monomers can then undergo polymerization and nucleation into 0D nanostructures[14]. When compared to dry torrefaction, HTC provides a more energy-efficient alternative with improved control over particle size and surface functionalization, thus providing the preferred approach for advanced nanofluid applications[6]. A detailed comparison between these strategies and their implications for CD synthesis is presented in Table 2.

Formation mechanisms and physicochemical properties of CDs

HTC-based synthesis of CDs involves a complex liquid-based route that differs significantly from conventional solid-state thermochemical processes. At subcritical water temperatures (180-250 °C), autogenous pressure is produced in the reactor. Formation of CDs involves four stages [Figure 2]: (i) hydrolysis of AFW macromolecules (carbohydrates, proteins, and lipids) into reactive monomers (e.g., glucose and amino acids); (ii) dehydration and fragmentation to form soluble furan-like intermediates; (iii) polymerization including cross-linking into polymer clusters that often proceed via Maillard-type interactions; and (iv) aromatization and nucleation leading to the formation of a stable graphitic core surrounded by a functionalized shell once critical supersaturation is reached[6,7,14]. Superior performance of AFW-based CDs as thermal nanofluid additives arises primarily due to their unique physicochemical properties. In terms of morphology, CDs appear as quasi-spherical structures with ultra-small diameters (usually less than 10 nm), resulting in a high surface-to-volume ratio for better energy transport[14].

A distinctive feature is their "self-passivated" surface chemistry derived from the nitrogenous and oxygenated species present in AFW. In addition to the good thermal conductivity, these nanomaterials have numerous hydroxyl (-OH), carboxyl (-COOH), and amino ($-NH_2$) groups on their surface, which render them extremely hydrophilic and highly dispersible in water[15]. The particles are more stable than traditional metallic nanoparticles due to the high density of surface groups; this results in excellent colloidal stability compared to other metallic nanoparticles, which often suffer from serious van der Waals forces and hence experience agglomeration and quick sedimentation in aqueous solutions under gravity[26].

A high absolute zeta potential value (typically

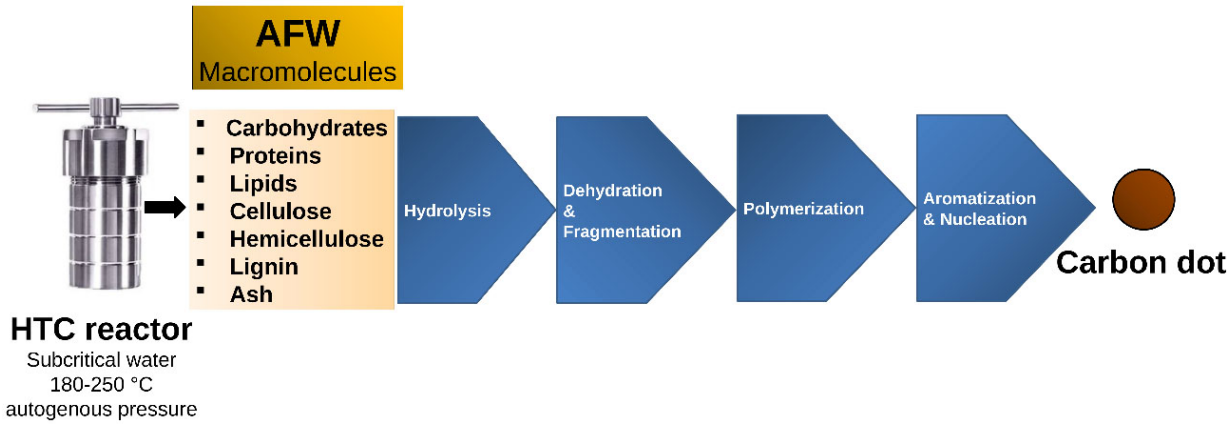

Figure 2. Thermochemical cascade of AFW via HTC. AFW: Agri-food waste; HTC: hydrothermal carbonization.

greater than |30| mV) enables the generation of strong electrostatic repulsion and steric hindrance between nanoparticles[26]. The nanoparticles do not undergo agglomeration and sedimentation processes. There is no need for the use of toxic or foaming surfactants[27]. This is an important feature of these nanoparticles in terms of engineering requirements for preparing high-performance thermal nanofluids because they do not exhibit any inconsistency in their thermophysical properties and do not pose the possibility of clogging in micro-channels in the case of the application of the fluids in continuous flow devices[26].

DATA-DRIVEN FRAMEWORK FOR INTELLIGENT CD SYNTHESIS AND NANOFLUID FORMULATION

Empirical trial-and-error to algorithmic optimization

The chemical synthesis of CDs from heterogeneous AFW using HTC involves complex non-linear reaction kinetics with multiple input variables acting on each other at the same time (e.g., temperature, residence time, biomass-to-water ratio, precursor composition). The parameters are typically varied individually through traditional OFAT screening, neglecting the simultaneous interaction between them. Such interactions are the most important factors controlling the final product quality[25]. Uncontrolled nanoparticle formation results in inconsistent core graphitization and varying surface passivation, hampering efforts to formulate consistent thermal nanofluids. The field needs to transition from trial-and-error to a data-driven approach. Several recent examples describe the use of computational analytics, statistical modeling, and machine learning (ML) to predictably engineer the interaction between precursors, processes, and properties within a limited parameter space[12,28].

However, extending the approach to larger untried precursor/process combinations has not yet been done, although it is a logical next step. The statistical DoE offers a middle ground before implementing ML models. Using the Taguchi orthogonal array method, the full factorial design (> 100 runs) can be reduced to a much smaller orthogonal design (< 20 runs). The approach eables identifying key HTC control factors such as temperature, residence time, and biomass-to-water ratio without excessive resources[8]. RSM approaches, namely the Box-Behnken and central composite designs, can generate response surfaces to map the relationship between precursor and process parameters to optimize the yield of CDs, their size (d < 10 nm), and the fluorescence quantum yield[10].

DoE creates the structure but does not go outside this range. ML can be relied upon to interpolate within this range. It has not been validated to extrapolate outside of this range. The review on AFW-HTC-CD papers discussed here suggests that it is still an open question whether ML can extrapolate.

Predictive modeling of thermophysical properties

ML models can be used in some cases for extensive experimentation or complex computational fluid dynamics simulations to predict the properties of nanofluids. One artificial neural network (ANN)

model was able to predict the thermal conductivity and dynamic viscosity of nanofluids with an accuracy of $R^2 > 0.95$ by training with only the concentration of CD, the type of base fluid, and the working temperature[9]. This result is specific to this dataset range but not a replacement for computational fluid dynamics or experimentation on any other dataset not tested. A small dataset for the laboratory testing typical of a new bio-refinery is best served by tree-based ensemble learning models such as random forest (RF) and extreme gradient boosting (XGBoost). The class of algorithms is better protected from overfitting[29]. The methods give information on the most important feature (such as hydrothermal reaction parameter control of the surface heteroatom functionalization group). This has a much greater impact on the colloidal stability of the resulting CDs than the variations inherent in the raw materials[29]. In addition to single-step predictions of properties, the evolution of computer-assisted design engineering points toward a new model: multi-objective optimization.

Table 3 gives an overview of recent literature and a cross-study map for a broad range of ML architectures applied to nanofluids, carbon precursors, target thermophysical or structural properties, and reported accuracies for those targets. The purpose is to show the engineering utility of these digital methods, not just their technical capabilities. In the last row, subcritical HTC of lignocellulosic biomass to hydrochar is included not as a carbon-dot characterization study, but as a process-level precedent for ML-guided HTC reactor optimization encompassing feedstock composition, reaction temperature, and residence time; accordingly, it does not evaluate carbon-dot synthesis or properties.

The accuracies in Table 3 are not directly comparable: reported n spans two orders of magnitude (20 to 2,500), and validation rigor varies from LOOCV on small samples to independent blind test sets on large ones. High R^2 at n < 100 (e.g., the active-learning study, n = 20-63) reflects efficient interpolation within a narrow, deliberately sampled region, not generalizable predictive power; only the large-sample rows (n > 1,000, external test sets) support a claim of robust performance. Reported R^2 values should therefore be read as an upper bound on in-domain accuracy, not as evidence of cross-precursor or cross-fluid transferability. Accordingly, Section 4 explores how these optimized CDs result in heat--transfer improvement of base fluids. Reported accuracies imply what was actually shown within each study's training domain. It is assumed that future studies may eventually develop a precursor-to-property ML framework that can be used with any desired AFW feedstock, and it is outside the scope of this review. Finally, Figure 3 wraps up the flowchart by illustrating the full pathway from AFW feedstock through DoE/RSM experimental design generation to ANN, tree-ensemble, and hybrid ML models and ending at the final optimized nanofluid formulation.

ADVANCED THERMAL NANOFLUIDS INTEGRATED WITH CDS

Dispersion of AFW-derived CDs into thermal base fluids leads to improved thermophysical properties. Traditional metallic or metal-oxide-based nanoparticles exhibit high densities, surface oxidation, and rapid settling due to gravity, whereas CDs have an entirely different synergistic mix. Table 4 shows that reported thermal conductivity enhancements can range from 11% up to 175%, depending on the base fluid composition, operating temperature, and CD loading[34,35].

Heat-transfer enhancement mechanisms

The mechanisms above are listed in decreasing order of evidence. To date, none have been identified experimentally for AFW-derived CD nanofluids. Thus, they are stated as contributors, but without specifying relative importance. The enhancement of thermal conductivity (k) in CD-based nanofluids extends beyond classic effective medium descriptions to a combination of multi-scale thermodynamic processes.

Brownian motion and micro-convection

Owing to their sub-10 nm, 0D structure, CDs exhibit rapid Brownian motion within the base fluid. It has been indicated that Brownian-driven micro-convection speeds up local heat and mass transfer[36]. This mechanism is commonly used to explain the temperature dependence of the measured thermal conductivity. Rather than being a leading explanation, the estimates indicate that this contribution may be secondary; in addition, the speed of diffusion for the nanoparticles directly through the liquid is an order of magnitude slower than the rate of thermal diffusion. Furthermore, the same temperature depen-

Table 3. Recent ML frameworks applied to CD characteristics and nanofluid thermophysical property prediction

Material / System	ML architecture	Key input features / dataset	Dataset size, validation & accuracy	Significance & ref.
Carbon nano-additives in thermal base fluids CNTs, graphene, CDs and hybrid nanomaterials dispersed in water, EG, and EG/water mixtures; renewable energy heat transfer applications	ANN (multi-layer perceptron), GMDH, SCG	• 5-7 core inputs: nanoparticle type, volume/weight concentration, base fluid type, operating temperature, particle size, aspect ratio, pH • 200-2,500 data points	• ***n*** = 200-2,500 data points (pooled across sub-models) • **Validation:** k-fold CV (k = 5 or 10); independent test set; MSE, MAE, R^2 • **Accuracy:** R^2 up to 0.9996 (ANN-SCG) for thermal conductivity and viscosity	Benchmarks ANN superiority over RSM and empirical correlations for multi-variable nanofluid property prediction[9]
Agri-waste biochar-derived CDs (banana peels)	ANN	• 5 features: CDs dosage, temperature, initial dye concentration, contact time, • ~ 43 data points	• ***n*** = 43 data points • **Validation:** 70/30 train-test split • **Accuracy:**R^2 > 0.982	The CDs have potential for dye removal[30]
Organic-precursor CDs (small-molecule, citric acid/urea/ethylenediamine)	ANN (classification + regression, two-stage/hybrid)	• Reaction method, solvent, pH, purification method; numerical: reaction temperature, reaction time; precursor composition (citric acid, urea, ethylenediamine, plus auxiliary reagents) • ***n*** = 407 literature-compiled data points (379 training / 28 external test)	• ***n*** = 407 data points • **Validation:** - • **Accuracy:** color classification accuracy = 94%; wavelength regression minimum MAE = 25.8 nm	Synthesis method and purification route are primary determinants of CD[31]
Full-color CQD synthesis, single precursor (2,7-naphthalenediol); hydrothermal/solvothermal	ML-integrated multi-objective optimization (MOO) using XGBoost regression	• 8 specific synthesis descriptors (temperature, time, catalyst type/volume, solvent type/volume, ramp rate, precursor mass); ~ 20-million-combination search space	• ***n*** = 63 • **Validation:** Iterative closed-loop retraining tracked via MSE • **Accuracy:** PLQY-MSE fell 0.45 → ≈ 0.1; PLQY > 60% across all 7 colors, 410-645 nm	Synthesis of full-color fluorescent CQDs with high PLQY exceeding 60% across all colors[32]
Biomass feedstocks under subcritical HTC treatment • Lignocellulose (wheat straw, corn cob, wood chips, rice husk, mixed wastes); coal-like hydrochar production	XGBoost, RF, and SVM (Grid-Search CV hyperparameter tuning; XGBoost outperformed others)	• 11 input features: volatile matter, ash, fixed carbon, C, H, O, N, HHV, reaction temperature (T), reaction time (RT), and solid-to-liquid ratio (SLR)	• ***n*** = 333 data points (approx.; multi-biomass, multi-condition) • **Validation:** 5-fold cross-validation and SHAP for model interpretation • **Accuracy:** R^2 from 0.825 to 0.985 (and RMSE from 1.119 to 5.426) across all algorithms. R^2 of 0.927 and an RMSE of 3.279 (XGBoost multi-task model)	Identifies ash content, temperature, and SLR as the three decisive process levers for hydrochar fuel quality and optimum condition[33]

ML: Machine learning; CD: carbon dot; ANN: artificial neural network; BO: Bayesian optimization; CV: cross-validation; *dp*: particle size; EG: ethylene glycol; GBDT: gradient boosting decision tree; GMDH: group method of data handling; GPR: gaussian process regression; CQD: carbon quantum dot; HHV: higher heating value; HTC: hydrothermal carbonization; LOOCV: leave-one-out CV; MAE: mean absolute error; MSE: mean squared error; MWCNT: multi-walled carbon nanotube; PLQY: photoluminescence quantum yield; QY: quantum yield; RF: random forest; SCG: scaled conjugate gradient; SLR: solid-to-liquid ratio; SVM: support vector machine; T: temperature; XGBoost: extreme gradient boosting; φ: volume fraction; RMSE: root mean square error.

dence can also arise from effects related to aggregation-driven percolation and the temperature dependence of the interfacial liquid layer. Distinguishing between these requires experiments that separate the particle size from the volume fraction for matching surface chemistry, which have not been performed to date for CDs.

Interfacial liquid layering and Kapitza resistance reduction

These oxygen-rich functional groups (-OH, -COOH) of biomass-derived CDs hydrogen-bond

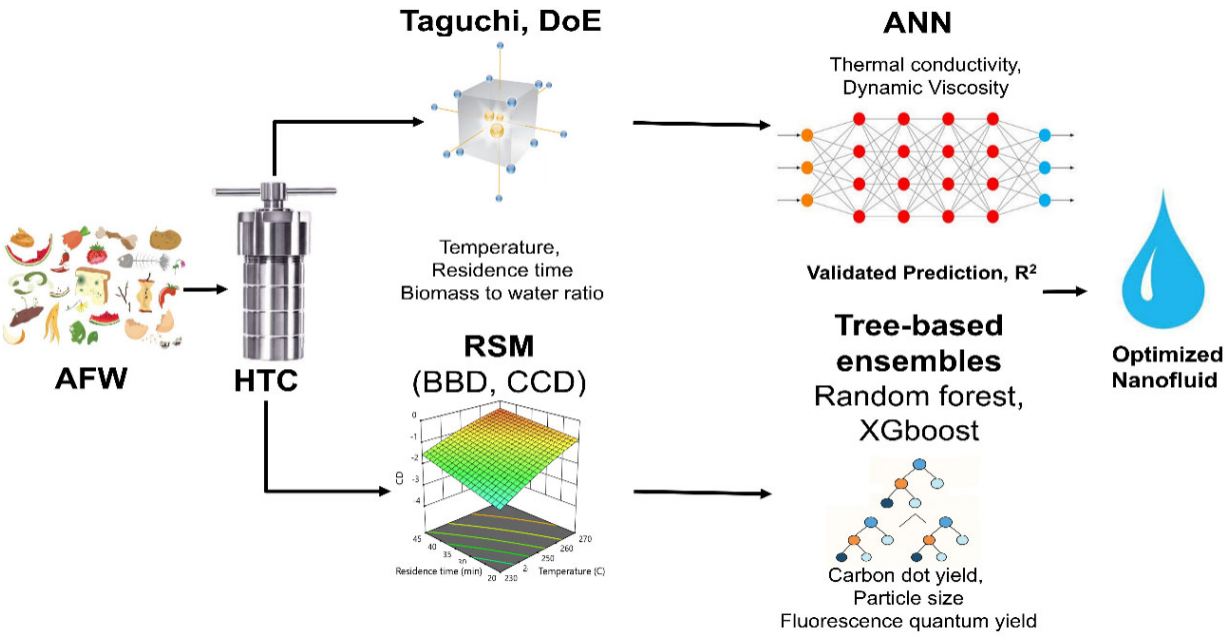

Figure 3. Schematic of the data-driven synthesis and nanofluid formulation framework integrating DoE, RSM, and ML approaches for AFW-derived carbon. DoE: design of experiment; ANN: artificial neural network; AFW: agri-food waste; HTC: hydrothermal carbonization; RSM: response surface methodology; BBD: Box-Behnken Design; CCD: Central Composite Design; XGBoost: extreme gradient boosting; ML: machine learning.

Table 4. Summary of reported TC enhancement in CD- and CNS-based nanofluids

Precursor	Base fluid	Conc. (wt.%)	Temp. (°C)	TC method & basis	Max. ΔTC (%)	ζ-potential (mV)	Ref.
Groundnut skin CD	EG; DI-EG (60:40)	0.01-0.10	30-80	Hamilton-Crosser model (theoretical); *vs.* base fluid	175 (EG, 0.1 wt.%, 80 °C)*	≈ 30	[27]
MXene + C-dot hybrid	Water (DI)	0.025-0.10	25-60	TPS (Hot Disk); *vs.* base fluid	50.0 (MXene alone) > 42.2 (hybrid) > 33.2 (C-dot alone)*	stable (no value given)	[35]
PEG-200 CD	PEG-200 (self-base)	not specified**	25-60	Not stated; *vs.* base PEG-200	11 (50 °C)*	not reported	[37]
Chemical-precursor CD	Water/EG blend	0.50	25-45	Not stated (experimental, method unspecified in source); *vs.* base fluid	21 (45 °C)*	−61.5	[38]
CuO-CD / Fe_3O_4-CD	Water (radiator coolant)	0.05-0.50	25-45	Not stated; *vs.* base fluid	25 (CuO-CD, 45 °C)*	not reported	[39]
PEG-200 CD (DASC)	PEG-200	not specified**	25-60	Not stated; *vs.* base PEG-200	11 (50 °C)*	not reported	[40]

ΔTC = maximum reported thermal conductivity enhancement relative to the unmodified base fluid, under the stated concentration and temperature. * No source in this table reports measurement uncertainty (standard deviation, confidence interval, or replicate count) for TC enhancement; values should be read as single-run or best-case figures as originally published. ** Concentration not specified in the cited source. 'Hamilton-Crosser model' denotes a theoretical mixture-conductivity correlation, not a direct experimental measurement, and is distinguished here from studies using instrumented methods (e.g., transient plane source/Hot Disk). TC: Thermal conductivity; CD: carbon dot; CNS: carbon nanosphere; EG: ethylene glycol; DASC: direct absorption solar collector; DI: deionized water; TPS: transient plane source; DFT: density functional theory; FESEM: field-emission scanning electron microscopy; FTIR: Fourier-transform infrared spectroscopy; HTC: hydrothermal carbonization; HTC coeff.: convective heat transfer coefficient; IL: ionic liquid; PEG-200: polyethylene glycol 200; N.R.: not reported; Raman: Raman spectroscopy; Re: Reynolds number; SPR: surface plasmon resonance; XRD: X-ray diffraction; ζ: zeta potential; η: photothermal conversion efficiency.

with polar base fluids to form a nanometer-thick ordered liquid layer at the solid-liquid interface that partially compensates for the phonon spectral mismatch and reduces the interfacial (Kapitza)

resistance[27]. This route relies on the correlations between surface oxygen content and enhancement and the results of molecular dynamics simulations of chemically similar functionalized carbon-water interfaces. However, it remains an unproven hypothesis in CD nanofluids. It would be desirable to confirm the mechanism directly via measurements of interfacial thermal conductance of AFW-derived CDs, e.g., using time-domain thermoreflectance. Yet, such measurements have yet to be performed. This mechanism can be considered to be only inferred[27,38].

Synergistic 0D/2D hybridization

By adding 2D nanomaterials such as MXene into the formulation, CDs may act as intercalating nano-spacers that prevent restacking of the nanosheets and maintain a percolating thermal network[35]. These results suggest an improvement in stability and interfacial interaction detected by Fourier Transform Infrared Spectroscopy (FTIR); however, it is important to note that no direct measurements of interlayer spacing were made under working conditions. The study also states that the enhancement in the case of the MXene/C-dot hybrid (42.2%) is less than that of pure MXene (50.0%)[35], suggesting that in this system the process of hybridization sacrifices peak conductivity for dispersion stability. The true value of the 0D/2D architecture is the balance between conductivity and stability during its lifetime. This is the exact information that is lost during short-term bench testing.

Broadband solar-thermal harvesting

Their unique optical properties such as their distinctive structural defects and surface states lead to a broad and strong absorption of light. These outstanding characteristics in photothermal conversion make them ideal candidates for direct absorption solar collectors, which can convert solar irradiation directly into local heat fast through non-radiative relaxation pathways[27].

Table 4 lists the values of the reported thermal conductivity enhancement of CD- and carbon nanosphere (CNS)-based nanofluids to date according to the precursors used, synthesis methods, and operation conditions. Biomass-based CD/CNS nanofluids present the best thermal conductivity enhancement (up to 175%) with a hybrid 0D/2D structure indicating the best balance between high conductivity and stability.

Colloidal stability and surface chemistry dynamics

One major challenge facing the commercialization of industrial nanofluids is long-term suspension stability, particularly in severe high-temperature cycling conditions. In this respect, food waste-derived CDs have been shown to greatly reduce this limitation due to their naturally self-passivated surfaces. The reported stability window is short compared to the industrial life span of multiple years (up to ~ 37 days) [34], and data on accelerated aging under realistic thermal cycling is still lacking. Yet, the high absolute zeta potential ($|\zeta| > 30$ mV, the conventional threshold for physical stability; $|\zeta| > 45$ mV indicates excellent stability) provided by the high density of carboxyl and amino groups originating from the protein- and carbohydrate-rich raw materials enables a strong electrostatic repulsion that leads to a high resistance to agglomeration even after prolonged heating-cooling cycles. Colloidal stability over 30 days has been reported for biomass-derived CD nanofluids (e.g., 37 days without sedimentation)[36]. This feature makes them an attractive alternative to conventional metallic nanoparticles for reducing clogging issues in heat-transfer loops.

In addition to these inherent advantages, CDs can be made suitable for operation in harsh environments through surface functionalization. Grafting with polyethylene glycol or ionic liquids can provide additional steric hindrance, locking colloidal stability. This modifies the rheology of the nanofluid toward non-Newtonian (shear-thinning) behavior, which should result in reduced pumping power compared to a Newtonian fluid with the same viscosity[27,31]. However, neither source has calculated the resulting change in pumping power or pressure drop due to these changes. Thus, it is assumed this is an additional advantage based on their description of the rheology. Finally, a common finding in the reviewed papers is that there is mixed reporting of thermal conductivity enhancements and viscosity penalties; while many give a value for one parameter, few give a value for both.

None of the papers included in this review gives a comparison of pumping power or pressure drop for the nanofluid alongside this information. Therefore, it is currently impossible to calculate the overall ther-

mohydraulic benefit of using AFW-derived CD nanofluids, the combination of the increase in heat-transfer rate and the associated increase in pumping power. This would control whether such systems can be used industrially. The published literature identifies this as a priority gap for future experimental work (Section **CONCLUSION**).

ENVIRONMENTAL IMPACT AND PRACTICAL CHALLENGES

The integration of food waste-derived CDs in the development of thermal nanofluids provides considerable improvement in terms of heat-transfer enhancement. However, before scaling up such promising lab achievements to an industrial level, it is important to evaluate their overall sustainability and scalability from a manufacturing point of view.

Life cycle assessment of agri-food waste-derived carbon dot synthesis

It is important to quantitatively show the "green" designation ascribed to biomass-derived CDs. Life cycle assessment (LCA), which complies with ISO 14040/14044, is a tool used to evaluate the impact on the environment from cradle-to-gate or cradle-to-grave. Fernandes *et al.*[41,42] performed LCA by employing four different methodologies for life cycle impact assessment (LCIA) calculations, namely ReCiPe, Greenhouse Gas Protocol, USEtox, and AWARE. Their results show that using high-yield hydrothermal methods does not provide any advantage in the environmental impact per gram when compared to low-yield conventional protocols.

The main concept is that the chemical precursor (i.e., citric acid and urea) is the largest impact contributor to global warming, fine particulate matter formation, and ecotoxicity, followed by the electricity consumed in operating the reactor. This justifies the use of AFW as an alternative to refined chemical precursors in CD synthesis. Crista *et al.*[43] replaced citric acid with spent coffee grounds in a one-pot thermal carbonization reaction (200 °C, 4 h; 10 kWh per batch (batch mass not reported); product diameter 2.1-3.9 nm; quantum yield 2.9%-5.8%). Their results suggest that such replacement can decrease environmental impacts for several categories based on the ReCiPe 2016 midpoint. They ascribe it solely to the elimination of the refined chemical precursor. In a study involving nitrogen-doped CDs synthesized hydrothermally from biomass-based xylose and commercial xylose (180 °C, 4 h), Rodríguez-Carballo *et al.*[44] concluded that the electric power and nitrogen precursor are both significant contributors to the total environmental impact. They did, however, highlight that the biomass-based xylose decreases the global warming contribution per kilogram of the product. Across all three datasets, substituting refined chemical precursors with AFW streams is the single highest-leverage environmental intervention in CD synthesis, independent of reactor configuration.

Environmental performance of CD-based nanofluids

If the system boundary is extended beyond the synthesis gate to include the whole life of the nanofluid, the benefit of AFW-derived CDs is further emphasized. In this context, Johny *et al.*[45] prepared fluorescent CDs using *Eucalyptus globulus* leaves via one-pot HTC (quantum yield 60.7%; excitation/emission 320/445 nm) and applied a cradle-to-gate LCA approach. Although the HTC process did not constitute the greatest environmental impact, the presence of citric acid as a co-functionalization reagent caused the main impact. Accordingly, the lowest burden was obtained with a fully AFW-derived CD in the absence of any other synthetic co-reagents. Dolgun *et al.*[46] measured the cumulative energy demand of the MWCNT/water and GNP/water nanofluids during their operational photovoltaic-thermal (PV/T) lifetime of 20 years.

It was shown that the improvements in thermal performance outweigh the greater energy inputs required for the synthesis of the nanofluids, and therefore, the resulting nanofluids are net-energy positive for their entire service life. This has also been highlighted by Sendão *et al.*[47], who examined TiO_2-CD nanocomposites, whereby the substitution of the synthetic precursor for the CDs with a biomass-derived equivalent resulted in a change in the major environmental hotspot from the photocatalyst manufacture to the electricity generation component. These results are confirmed by recent reviews by Razzaq *et al.*[48] on 30+ LCA studies carried out on nanofluids. Here, it was noted that up to 80% of the cradle-to-gate impact of nanofluids arises from the preparation of the NPs. However, once a long service phase is considered and waste-based materials replace pure refined feedstocks, the

percentage contribution falls dramatically.

Critical data gaps and scalability constraints

While this information is clear from the direction of the LCA results (Sections **Life cycle assessment of agri-food waste-derived carbon dot synthesis** and **Environmental performance of CD-based nanofluids**), there are still two factors that limit the quantitative reliability of the sustainability claim. First, none of the published LCA studies cover the whole lifecycle including the service life performance and/or the fate of the materials after their use phase has been included in an LCA analysis. To date, there is no published cradle-to-grave assessment of any AFW-derived CD nanofluid. Second, all the studies have used bench-scale batch autoclave data (< 1 L) as the sole source of process data (there is no LCI data available for larger scales). This is not representative of the actual industrial scale process, where continuous flow HTC is employed (> 100 L).

The change from bench-scale batch autoclave reactors to pilot-scale continuous flow HTC reactors influences the physical parameters of the HTC process. At bench scale, the autoclave reactions are carried out in near-isothermal conditions, whereas at pilot scale, due to the larger cross-sectional area, significant thermal gradients (15-30 °C) develop, leading to zones with lower temperatures (below the critical CD nucleation temperature) in the reactor[6,7]. This will result in an increase in the size distribution, less overall graphitization, and lower fluorescence quantum yield than expected based on the small-batch autoclave reaction times. Malika *et al.*[49] reported a similar trend for green synthesized iron-oxide nanoparticles, where they scaled up from 0.5 L to 20 L batches, which resulted in a 40% shift in the size distribution.

The lack of a reliable inventory compounds these issues. First, there is no standardized Life Cycle Inventory (LCI) data for HTC-specific unit operations, reactor pressurization, autogenous pressure maintenance, dialysis purification, or centrifugal separation. The lack of standardized LCI data for HTC unit operations is cited by De Matteis *et al.*[50] as the major reason why comparative LCA for plant-derived CDs is difficult, with proxy data for chemically dissimilar processes potentially assigning the wrong dominant impact category altogether. There is also a strong publication bias in favor of reporting only synthesis runs where everything goes according to plan. Datasets from syntheses almost always omit failed runs and off-specification product. These will likely constitute the majority of data from an industrial quality-control record[26]. A database compiled using this approach will underestimate the variability and the cost in terms of energy and materials associated with the process.

The most important knowledge gaps to be addressed include

• No cradle-to-grave LCA: Service-life thermal performance offsets (proven for MWCNT/water nanofluids over a 20-year PV/T lifespan by Dolgun *et al.*[46]) have not yet been quantified for CD-based systems, meaning that their net contribution to environmental balance has not been determined.

• No pilot-scale HTC life cycle inventory: There is no available data for energy and mass balances of continuous-flow reactors. Batch-to-batch variability, heat-recovery efficiency, and cleaning-in-place water demand at scale are all unknown.

• Publication-biased training data: ML models and LCA inventories use only successful, optimized syntheses as training examples, leading to overestimates of expected yield and quality consistency because negative and sub-optimal results are not considered.

• Undefined end-of-life profile: No data on ecotoxicology, biodegradability, or recovery efficiency of dispersed CDs in spent heat-transfer fluid has been evaluated. This can impede industrial deployment in most jurisdictions.

Until such a data infrastructure is established, sustainability claims for AFW-derived CD thermal nanofluids remain directionally supported but insufficiently evidenced for regulatory or investment-grade decision-making. The four gaps identified above, publication-biased training data, absent pilot-scale HTC inventories, missing cradle-to-grave LCA, and an undefined end-of-life profile, are addressed by the consolidated research priorities in Section **CONCLUSION**. The research priorities identified here inform the recommendations in Section **CONCLUSION** directly.

CONCLUSION

The complexity of AFW is turned into an engineering strength. The mixture of carbohydrates, proteins, and lipids can provide all the building blocks to prepare self-passivated CDs through HTC. The heteroatom nitrogen and oxygen elements provided by the protein and carbohydrate components eliminate the need for post-functionalization and thus directly address the two major obstacles for the application of conventional carbon nanomaterial-based thermal fluids (i.e., cost and toxicity). The advantages are further enhanced by the data-driven synthesis strategy introduced in Section **DATA-DRIVEN FRAMEWORK FOR INTELLIGENT CD SYNTHESIS AND NANOFLUID FORMULATION**. The transition from traditional trial-and-error approaches to data-driven algorithms represents a game-changing conceptual advancement for the upscaling of material development. By incorporating ML architectures into the synthesis route, scientists can understand the non-linear behavior of the HTC reactions. The combined power of these computational strategies will allow the pre-design ("inverse design") of targeted physical performance characteristics (e.g., target thermal conductivity and optimal dynamic viscosity) before the actual synthesis process is physically implemented.

This holistic strategy can not only address the global crisis of organic waste but also provide a viable pathway for future large-scale implementation of smart AFW-to-nanomaterials strategies based on sustainable principles. Such integration between smart AFW-to-nanomaterials and artificial intelligence would enable the application of high-performance self-stabilized thermal nanofluids for next-generation applications such as heat exchangers, energy storage devices, and solar-thermal collectors.

These findings suggest that the following research priorities should be addressed to fill gaps in the knowledge as outlined in Section **Critical data gaps and scalability constraints**: (1) a publicly available, standardized database of AFW-HTC-CD synthesis results including negative results should be developed to resolve the problem of training data shortage for ML models; (2) full LCA assessments of continuous-flow pilot-scale HTC systems need to be carried out to evaluate the environmental and economic feasibility of AFW-derived CD nanofluids compared with traditional alternatives; (3) experimental nanofluid data obtained from real solar-thermal collector test rigs under dynamic operating conditions should be used to verify the thermophysical properties predicted by ML; and (4) the fate and ecotoxicity of CD nanoparticles in end-of-life heat transfer fluid disposal pathways need to be explored to develop regulatory frameworks for industrial applications.

DECLARATIONS

Authors' contributions

Conception, review design, and writing of the original draft: Samsalee, N.; Manatura, K.

Agri-food waste characterization, Section **Compositional synergy: carbohydrates, proteins, and lipids as precursors data**, and Table 1 compilation: Samsalee, N.; Sothornvit, R.

Hydrothermal carbonization methodology review and Sections **Comparative analysis of dry torrefaction *vs.* HTC** and **Formation mechanisms and physicochemical properties of CDs**: Manatura, K.

ML framework review (Section **DATA-DRIVEN FRAMEWORK FOR INTELLIGENT CD SYNTHESIS AND NANOFLUID FORMULATION**) and data-driven analysis: Manatura, K.

Manuscript discussion and revision: Samsalee, N.; Sothornvit, R.; Manatura, K.

Critical revision, supervision, and correspondence: Manatura, K.

All authors approved the final version of the manuscript.

Availability of data and materials

Not applicable.

AI and AI-assisted tools statement

During the preparation of this manuscript, the authors used Google Gemini Pro (version 3.1, released 2026-02-19) to generate individual graphical elements (icons representing molecular structures and reaction stages) for Figures 2 and 3. The AI tool did not influence the study design, data collection, analysis, interpretation, or the scientific content of the work. All authors take full responsibility for the accuracy, integrity, and final content of the manuscript.

Financial support and sponsorship

The work is financially supported by the Science Research and Innovation Fund, Agreement No. FF69/NKR/064.

Conflicts of interest

All authors declared that there are no conflicts of interest.

Ethical approval and consent to participate

Not applicable.

Consent for publication

Not applicable.

REFERENCES

1. Kassim, F. O.; Thomas, C. P.; Afolabi, O. O. Integrated conversion technologies for sustainable agri-food waste valorization: a critical review. *Biomass. Bioenerg.* **2022**, *156*, 106314. DOI
2. Kumari, R.; Singh, A.; Sharma, R.; Malaviya, P. Conversion of food waste into energy and value-added products: a review. *Environ. Chem. Lett.* **2024**, *22*, 1759-90. DOI
3. Jaroenkietkajorn, U.; Gheewala, S. H.; Mungkung, R.; et al. Challenges and opportunities of bio-circular-green economy for agriculture. *Circ. Econ. Sust.* **2024**, *4*, 1729-50. DOI
4. Navidfar, A.; Peker, M. I.; Budak, E.; Unlu, C.; Trabzon, L. Carbon quantum dots enhanced graphene/carbon nanotubes polyurethane hybrid nanocomposites. *Compos. Part. B-Eng.* **2022**, *247*, 110310. DOI
5. Huang, Z.; Ren, L. Large scale synthesis of carbon dots and their applications: a review. *Molecules* **2025**, *30*, 774. DOI
6. Wu, S.; Wang, Q.; Fang, M.; et al. Hydrothermal carbonization of food waste for sustainable biofuel production: advancements, challenges, and future prospects. *Sci. Total. Environ.* **2023**, *897*, 165327. DOI
7. Zhang, J.; Zhou, Q.; Xia, A.; et al. Co-producing carbon dots and hydrochars via hydrothermal carbonization of microalgae: transformation mechanisms and reaction kinetics. *Bioresour. Technol.* **2026**, *439*, 133299. DOI
8. Chanpee, S.; Jadsadajerm, S.; Manatura, K.; et al. Optimization of hydrothermal carbonization of Rhizoclonium riparium macroalgae using response surface methodology for high-performance solid biofuel production. *Biomass. Conv. Bioref.* **2026**, *16*, 7039. DOI
9. Sharma, P.; Said, Z.; Kumar, A.; et al. Recent advances in machine learning research for nanofluid-based heat transfer in renewable energy system. *Energy. Fuels.* **2022**, *36*, 6626-58. DOI
10. Manatura, K.; Chalermsinsuwan, B.; Kaewtrakulchai, N.; Chao, Y.; Li, Y. Co-torrefaction of rice straw and waste medium density fiberboard: a process optimization study using response surface methodology. *Results. Eng.* **2023**, *18*, 101139. DOI
11. Awogbemi, O.; Adeleye, S. A.; Ojo, A. A. Experimental evaluation of proximate, ultimate, heating values, and structural composition of selected crop shells. *Discov. Sustain.* **2025**, *6*, 2016. DOI
12. Ren, J.; Opoku, H.; Tang, S.; Edman, L.; Wang, J. Carbon dots: a review with focus on sustainability. *Adv. Sci. (Weinh).* **2024**, *11*, e2405472. DOI PubMed PMC
13. Sulaeman, A. P.; Gao, Y.; Dugmore, T.; Remón, J.; Matharu, A. S. From unavoidable food waste to advanced biomaterials: microfibrilated lignocellulose production by microwave-assisted hydrothermal treatment of cassava peel and almond hull. *Cellulose* **2021**, *28*, 7687-705. DOI
14. Manatura, K. Inert torrefaction of sugarcane bagasse to improve its fuel properties. *Case. Stud. Therm. Eng.* **2020**, *19*, 100623. DOI
15. Lee, K.; Gabriela, S.; Chen, W.; Ong, H. C.; Rajendran, S.; Tran, K. Co-torrefaction and synergistic effect of spent coffee grounds and tea waste for sustainable waste remediation and renewable energy. *Renewable. Energy.* **2024**, *233*, 121181. DOI
16. Hamid, M.; Kaus, N. H. M.; Isnaeni, I.; et al. Development of carbon nanodots from durian waste incorporated with first-row transition metals for efficient degradation of microplastics in oral care products. *Diam. Relat. Mater.* **2026**, *162*, 113238. DOI
17. Andrade, L.; Barrozo, M.; Vieira, L. Thermo-chemical behavior and product formation during pyrolysis of mango seed shell. *Ind. Crops. Prod.* **2016**, *85*, 174-80. DOI
18. Kaniapan, S.; Suhaimi, H.; Hamdan, Y.; Pasupuleti, J. Experiment analysis on the characteristic of empty fruit bunch, palm kernel shell, coconut shell, and rice husk for biomass boiler fuel. *JMES* **2021**, *15*, 8300-9. DOI
19. Zhang, L.; Wang, Y.; Liu, W.; Ni, Y.; Hou, Q. Corncob residues as carbon quantum dots sources and their application in detection of metal ions. *Ind. Crops. Prod.* **2019**, *133*, 18-25. DOI
20. Masroor, A.; Umar, M. Z.; Ashraf, M.; et al. Demineralization and torrefaction of mango peel waste: effect of process parameters. *Biomass. Conv. Bioref.* **2026**, *16*, 7013. DOI
21. Behera, U. S.; Poddar, S.; Byun, H. Pyrolysis of orange peel waste to pyrofuels and pyrochar: optimization and techno-economic insights for industrial scale-up. *RSC. Sustainability.* **2025**, *3*, 5527-55. DOI
22. Wijaya, C. J.; Saputra, S. N.; Soetaredjo, F. E.; et al. Cellulose nanocrystals from passion fruit peels waste as antibiotic drug carrier. *Carbohydr. Polym.* **2017**, *175*, 370-6. DOI

23. Islam, M. A.; Akber, M. A.; Limon, S. H.; Akbor, M. A.; Islam, M. A. Characterization of solid biofuel produced from banana stalk via hydrothermal carbonization. *Biomass. Conv. Bioref.* **2019**, *9*, 651-8. DOI
24. Kumar J, Kavitha G, Arulmozhi R, Arul V, Singaravadivel S, Abirami N. Green sources derived carbon dots for multifaceted applications. *J. Fluoresc.* **2021**, *31*, 915-32. DOI PubMed
25. Cai, D.; Zhong, X.; Xu, L.; et al. Biomass-derived carbon dots: synthesis, modification and application in batteries. *Chem. Sci.* **2025**, *16*, 4937-70. DOI PubMed PMC
26. Seifikar, F.; Azizian, S. Super-stable carbon quantum dots nanofluid for efficient solar-thermal conversion. *Energy. Convers. Manage.* **2021**, *228*, 113675. DOI
27. Bijapur, K.; Mandal, S.; Siddheshwar, P. G.; Bose, S.; Hegde, G. Experimental investigation of a biomass-derived nanofluid with enhanced thermal conductivity as a green, sustainable heat-transfer medium and qualitative comparison via mathematical modelling. *Nanoscale. Adv.* **2024**, *6*, 4944-55. DOI PubMed PMC
28. Liu, Q.; Chen, H.; Mi, R.; et al. Biomass-derived carbon dots: preparation, properties, and applications. *Nanomaterials. (Basel).* **2025**, *15*, 1279. DOI PubMed PMC
29. Meng, W.; Bai, X.; Wang, B.; Liu, Z.; Lu, S.; Yang, B. Biomass-derived carbon dots and their applications. *Energy. Environ. Mater.* **2019**, *2*, 172-92. DOI
30. Shahraki H, Ahmad A, Qurtulen, Bushra R, Momina. Biomass derived carbon dots for enhanced wastewater remediation: ANN-optimized synthesis and cellular imaging applications. *Inorg. Chem. Commun.* **2024**, *166*, 112690. DOI
31. Senanayake, R. D.; Yao, X.; Froehlich, C. E.; et al. Machine learning-assisted carbon dot synthesis: prediction of emission color and wavelength. *J. Chem. Inf. Model.* **2022**, *62*, 5918-28. DOI PubMed PMC
32. Guo, H.; Lu, Y.; Lei, Z.; et al. Machine learning-guided realization of full-color high-quantum-yield carbon quantum dots. *Nat. Commun.* **2024**, *15*, 4843. DOI PubMed PMC
33. Liu, Q.; Zhang, G.; Yu, J.; et al. Machine learning-aided hydrothermal carbonization of biomass for coal-like hydrochar production: Parameters optimization and experimental verification. *Bioresour. Technol.* **2024**, *393*, 130073. DOI
34. Wang, H.; Chen, X. A comprehensive review of predicting the thermophysical properties of nanofluids using machine learning methods. *Ind. Eng. Chem. Res.* **2022**, *61*, 14711-30. DOI
35. Sreekumar, S.; Ganguly, A.; Khalil, S.; et al. Thermo-optical characterization of novel MXene/carbon-dot hybrid nanofluid for heat transfer applications. *J. Clean. Prod.* **2024**, *434*, 140395. DOI
36. Gonçalves, H. M. R.; Pereira, R. F. P.; Lepleux, E.; et al. Non-Newtonian thermosensitive nanofluid based on carbon dots functionalized with ionic liquids. *Small* **2020**, *16*, e1907661.
37. Zhou, J.; Li, X.; Chen, W.; Cui, R.; Wu, X. Investigation on the photothermal performance of carbon quantum dots nanofluid with high-stability. *Diam. Relat. Mater.* **2022**, *128*, 109233. DOI
38. Askari, S.; Ettefaghi, E.; Rashidi, A.; et al. Ultra-stable nanofluid containing functionalized-carbon dots for heat transfer enhancement in water/ethylene glycol systems: experimental and DFT studies. *Energy. Rep.* **2021**, *7*, 4222-34. DOI
39. Bijapur, K.; Mandal, S.; Siddheshwar, P. G.; Bose, S.; Hegde, G. Unlocking efficiency: experimental and theoretical insights into biomass-derived carbon nanofluids with enhanced thermal conductivity. *Nanoscale* **2025**, *17*, 10239-49. DOI PubMed
40. R. Gonçalves H, Neves SAF, Duarte A, de Zea Bermudez V. Nanofluid based on carbon dots functionalized with ionic liquids for energy applications. *Energies* **2020**, *13*, 649. DOI
41. Fernandes, S.; Esteves, da. Silva. J. C. G.; Pinto, da. Silva. L. Comparative life cycle assessment of high-yield synthesis routes for carbon dots. *NanoImpact* **2021**, *23*, 100332. DOI PubMed
42. Fernandes, S.; Esteves, da. Silva. J. C. G.; Pinto, da. Silva. L. Life cycle assessment-based comparative study between high-yield and “standard” bottom-up procedures for the fabrication of carbon dots. *Materials. (Basel).* **2022**, *15*, 3446. DOI PubMed PMC
43. Crista, D. M. A.; El, Mragui. A.; Algarra, M.; Esteves, da. Silva. J. C. G.; Luque, R.; Pinto, da. Silva. L. Turning spent coffee grounds into sustainable precursors for the fabrication of carbon dots. *Nanomaterials. (Basel).* **2020**, *10*, 1209. DOI PubMed PMC
44. Rodríguez-Carballo, G.; Moreno-Tost, R.; Fernandes, S.; et al. Nitrogen doped carbon dots as a photocatalyst based on biomass. A life cycle assessment. *Journal. of. Cleaner. Production.* **2023**, *423*, 138728. DOI
45. Johny, A.; Pinto, da. Silva. L.; Pereira, C. M.; Esteves, da. Silva. J. C. G. Sustainability assessment of highly fluorescent carbon dots derived from eucalyptus leaves. *Environments* **2024**, *11*, 6. DOI
46. Dolgun, G. K.; Koşan, M.; Kayfeci, M.; Georgiev, A. G.; Keçebaş, A. Life cycle assessment and cumulative energy demand analyses of a photovoltaic/thermal system with MWCNT/water and GNP/water nanofluids. *Processes* **2023**, *11*, 832. DOI
47. Sendão, R. M. S.; Esteves, da. Silva. J. C. G.; Pinto, da. Silva. L. Comparative life cycle assessment of the fabrication of visible-light-driven photocatalytic TiO_2 - carbon dots nanocomposites for wastewater treatment. *NanoImpact* **2025**, *38*, 100556. DOI PubMed
48. Razzaq, I.; Xinhua, W.; Rasool, G.; et al. Nanofluids for advanced applications: a comprehensive review on preparation methods, properties, and environmental impact. *ACS. Omega.* **2025**, *10*, 5251-82. DOI PubMed PMC

49. Malika, M.; Jhadav, P. G.; Parate, V. R.; Sonawane, S. S. Synthesis of magnetite nanoparticle from potato peel extract: its nanofluid applications and life cycle analysis. *Chem. Pap.* **2023**, *77*, 1081-94. DOI

50. De, Matteis. V.; Baglivo, C.; Tamborino, S.; et al. Structure-optical properties and sustainability assessment of carbon dots derived from *Laurus nobilis* leaves. *Applied. Nano.* **2025**, *6*, 19. DOI